Repairable System Analysis of the Radioactive Ventilation Gas Monitors at CERN from Field Data

Saskia Hurst[1], Hamza Boukabache[2], and Daniel Perrin[3]

[1,2,3]*CERN, Geneva, 1211, Switzerland*

saskia.kristina.hurst@cern.ch
hamza.boukabache@cern.ch
daniel.perrin@cern.ch

ABSTRACT

CERN has the legal obligation to protect the public and the people working on its site from any unjustified exposure to ionizing radiation. Therefore, several monitoring systems are operated at CERN to evaluate the radiological impact of CERN's accelerators and installations by active monitoring. Having highly reliable and available monitoring systems is hence a crucial factor to ensure a safe operation and steady availability of the accelerator. Besides designing reliable systems or implementing a condition-based maintenance strategy, the analysis of field data also helps to achieve these high reliability and availability goals. To decide, whether a system should be replaced or to estimate its situation on its lifetime curve, the analysis of field data is appropriate. This paper will present how failure data from maintenance interventions on the example of the Ventilation Gas Monitors (VGM) are used to estimate the system lifetime, failure rate and optimal point for exchange. A power law process is used to model the parametric growth curve of the number of failures and the Nelson-Aalen estimator is employed to model the non-parametric growth curve of the number of failures for repairable systems. The power law model is extrapolated and enhanced by its failure costs to make estimations about the necessary budget in the future and the optimal time for exchange. Additionally, confidence bounds and goodness-of-fit tests are included to evaluate the precision of the prediction. Taking advantage of open source software, a model with R language is established for all the calculations.

The first chapter of this paper gives an introduction to the topic. The second chapter outlines the functioning, structure and lifetime requirements of the VGM system and presents its collected failure data. The third chapter specifies the mathematical background for repairable system analysis, how the parameters are calculated with maximum likelihood estimation and describes the implementation of the Cramér-von Mises criterion and confidence bounds as goodness-of fit tests. The fourth chapter presents the results for the VGM system. The last chapter contains a conclusion and an outlook.

1. INTRODUCTION

Data collected from systems in the field are called fielded systems data and are analogous to warranty data. Fielded systems can be categorized as either non-repairable systems or repairable systems. When these systems are safety critical or customer products, it is often of interest to determine its reliability characteristics like the expected number of failures during the warranty period, maintaining a minimum mission reliability, evaluating the rate of wear-out, determining when to replace and overhaul the system or to minimize its life cycle costs.

For cost reasons most complex systems are repaired and not replaced after each failure. Therefore, it is not possible to model these systems with the Weibull distribution, which is used to model non-repairable systems, but instead to use a process. The most commonly applied one is the power law process, which will also be used in this paper (ReliaSoft, 2010).

2. THE VGM SYSTEM

The Ventilation Gas Monitors (VGM) at CERN aim at monitoring activity concentrations of short-lived radioactive gases and are equipped with alarm and interlock functions. Several units (39) are installed all over the CERN area since 2008 with the start of the Large Hadron Collider (LHC) to continuously perform the measurements and ensure, amongst other monitoring systems, the compliance with defined radiation dose levels.

Figure 1 shows a VGM station, consisting of a measurement chamber, a data processing box, a power supply box, a signal processing, a monitoring station (PLC and panel PC), an airflow system (pump, valves, float flow meter) and the treatment box.

Figure 1. Ventilation Gas Monitor (VGM) (Perrin, 2018).

2.1. Structure and Measurement Principle

Radioactive gases continuously flow through a measurement chamber equipped with two passively implemented planar silicon detectors (PIPS) by CANBERRA. The first detector is facing the gases, while the second, placed atop, serves as a guard detector for active ambient background compensation. The radionuclides of interest are short-lived, medium to high energy beta particles emitters (^{11}C, ^{13}N, ^{14,15}O, ^{41}Ar). In addition to pulse height discrimination (cut-off energies), unwanted signal rejection is made by mean of a thin foil placed in front of the measurement detector, that shields very low energy beta and all alpha particles, respectively emitted by tritium and natural radon progenies. The treatment box (in the center of the VGM`s information processing) receives the analogue pulses from the diodes and transmits the logic pulses to the data processing box. The activity concentration is derived from the measured net count rate, by mean of a calibration coefficient initially determined by Monte-Carlo simulations validated by measurements (Ferragut, 2005). Because the system is not capable to distinguish the respective contributions of the aforementioned radionuclides (beta particles, continuous and overlapping spectra), the most penalizing calibration coefficient is conservatively used (^{41}Ar).

Figure 2 shows the schematic functioning of a VGM.

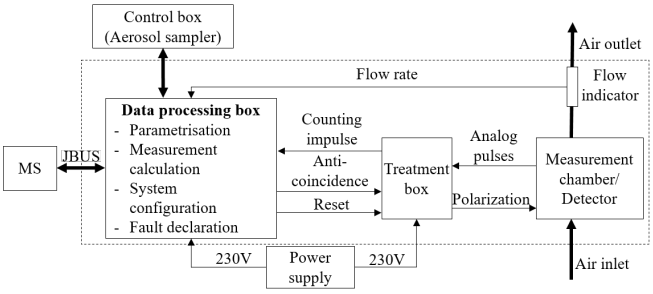

Figure 2. Schematic Structure of a VGM.

2.2. Lifetime Requirements

As the VGM system is procured from an external company and no longer available on the market, it could be replaced partially by an in-house developed monitoring system at the end of its lifetime. The VGM system is used since 2008 with the start of the Large Hadron Collider (LHC) and therefore field data collected for 12 years are available. This can be used to perform a reliability analysis to minimize its maintenance costs, having sufficient spare parts and complying with the required Safety Integrity Level (SIL) 2. The field data are maintained in a database which contains all failures, including the failure type, date of occurrence, repair costs and serves as basis for the analysis.

2.3. Failure Data

At CERN all maintenance data concerning the VGM are stored manually in a ©SharePoint database and automatically into REMUS Supervisory, Control and Data Acquisition system (SCADA) developed at CERN. REMUS contains all kind of data such as measurements, calibration, configurations and some hardware failures. In contrast ©SharePoint was used for on field data collection. It contains only relevant hardware and software failures. Each failure is specified and the type of repair is mentioned. As the maintenance is done by an external contracting company, each repair can be linked to a separate invoice. Therefore, for each failure type the costs are also known.

Table 1 contains a summary of the failure types that have occurred (extracted and summarized from ©SharePoint).

Not all failures are relevant for the analysis; hardware-setting failures are for example purely related to the user and not the equipment. The power supply failure is a concrete wear-out failure and considered separately. In addition, detector failures are also considered separately, as the detector is not maintained by the same manufacturer. It is a separate part of the VGM. After discussion with experts, amplifier failures, measurement system failures, connector failures and EMC issues are considered together for the analysis.

The failure data are right-censored, as the systems are only observed until a certain time.

Table 1. Failure Data.

Failure type	Failure details	Fault correction
Connector failure	Clamp-; crimp-connection, Vibration, broken socket	Tightening of connections, cleaning, replacement of sockets/cables
Detector failure		Replacement
Amplifier failure	Preamplifier, microprocessor, comparator broken	Replacement
Measurement system failure	Fuse, microprocessor	Replacement
EMC issues	Electrical noise on measurement,	Isolating transformer, high-pass filter, ferrite core
Hardware settings		Adjustment of the settings
Power supply failure		Replacement

Non-censored data in contrary would be available when a unit would be taken out of operation after a failure. In the example of the VGMs, the data are time-censored (until the point when the analysis was made). If the observation would stop after a predefined number of failures, the data would be called failure-censored (Birolini, 2017).

3. APPROACH RELIABILITY ANALYSIS FROM FIELD DATA

For repairable systems analysis, the R software was used to process the data coming from ©SharePoint, REMUS and invoices from the contracting companies.

3.1. Repairable System Analysis

Generally, in survival theory, the Weibull distribution is used to model the lifetime of non-repairable systems. To address the reliability characteristics of complex repairable systems, a process, most commonly the power law model is used instead of a distribution. The power law model is a parametric model and appropriate to model systems with "minimal repair". This concept means that a failed system is repaired in a way just to get it operational again. If a system has many failure modes, the repair of a single failure does not improve the system reliability compared to its reliability before the occurrence of the failure. In this case, the sequence of failures at the system level follows a non-homogeneous Poisson process (NHPP) (ReliaSoft, 2010).

In case the system is overhauled after a certain period, the reliability is greatly improved afterwards which can also be implemented in the power law model. The power law model with the mean cumulative number of failures *MCF(t)* is described by Eq. (1) and its intensity function *f(t)* (failure rate) in Eq. (2).

$$MCF(t) = \hat{\lambda} \cdot t^{\hat{\beta}} \tag{1}$$

$$f(t) = \hat{\lambda} \cdot \hat{\beta} \cdot t^{(\hat{\beta}-1)} \tag{2}$$

Herein $\hat{\lambda}$ is the scale estimate and $\hat{\beta}$ is the shape estimate.

A special case for the power law model is when there is no change in the intensity function ($\beta=1$). This is referred to a homogenous Poisson process (HPP). When $\beta<1$, the system is improving over time, in contrary to $\beta>1$ where the system is degrading over time.

This behavior is visualized in Figure 3. The MCF (Mean Cumulative Function) of the power law process for three different shape parameters is plotted.

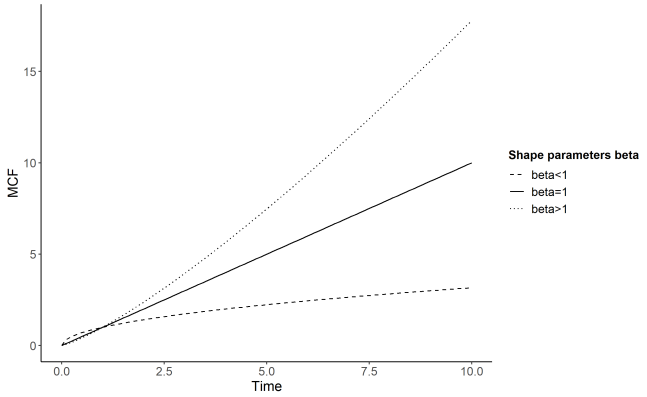

Figure 3: MCF for Different Shape Parameters.

Reliability growth curves give the mean number of cumulative failures over time per unit and help to establish how often a system requires maintenance and the number of necessary replacement items in inventory. It can also indicate if the system is performing at an acceptable level. From the graphs, the trend of the process can be derived by its shape parameters and the rate of occurrence of failure over time can be deviated and compared to the SIL. The parameters of the power law model are estimated by the maximum likelihood method.

Eq. (3) and Eq. (4) present the maximum likelihood estimators of the scale parameter $\hat{\lambda}$ and the shape parameter $\hat{\beta}$, whereas K is the number of systems and the q^{th} system is observed continuously from time S_q to time T_q (q=1, 2, ..., K). N_q is the number of observed failures during the period $[S_q, T_q]$ by the q^{th} system. $X_{i,q}$ is the age of this system at the i^{th} occurrence of failure (i=1, 2, …, N_q). If $X_{i,q}=T_q$ the data on this system are failure terminated; if $X_{i,q}<T_q$ the system is time terminated (ReliaSoft, 2010).

$$\hat{\lambda} = \frac{\sum_{q=1}^{K} N_q}{\sum_{q=1}^{K} \left(T_q^{\hat{\beta}} - S_q^{\hat{\beta}} \right)} \tag{3}$$

$$\hat{\beta} = \frac{\sum_{q=1}^{K} N_q}{\hat{\lambda} \sum_{q=1}^{K} \left[T_q^{\hat{\beta}} \ln(T_q) - S_q^{\hat{\beta}} \ln(S_q) \right] - \sum_{q=1}^{K} \sum_{i=1}^{N_q} \ln(X_{i,q})} \tag{4}$$

If all units have the same starting point ($S_1=S_2=\ldots=S_q=0$) and end-point ($T_1=T_2=\ldots=T_q=0$), the equations can be simplified to Eq. (5) and Eq. (6).

$$\hat{\lambda} = \frac{\sum_{q=1}^{K} N_q}{KT^{\beta}} \tag{5}$$

$$\hat{\beta} = \frac{\sum_{q=1}^{K} N_q}{\sum_{q=1}^{K}\sum_{i=1}^{N_q} ln\left(\frac{T}{X_{i,q}}\right)} \tag{6}$$

By extrapolating the parametric growth curve, estimations about the amount of failures and therefore the necessary spare parts in the future can be made. The growth curve of the cumulative number of failures of the VGM is also used to calculate future repair costs by enhancing the graph by its average repair costs. To minimize costs and optimize the replacement, the reliability growth curves of the VGM also serve as basis to calculate the optimal point of exchange.

Failure data can also be plotted by the Nelson-Aalen estimator, which is a non-parametric estimator of the cumulative number of failures *H(t)* for non-censored, censored and incomplete data. Eq. (7) shows the calculation with d_i number of events (failures) at t_i and n_i the total individuals at risk at t_i (Nelson, 2003).

$$H(t) = \sum_{t_i \le t} \frac{d_i}{n_i} \tag{7}$$

This model is used additionally to the power-law model, but cannot be used for extrapolation.

3.2. Evaluation of the Model Prediction

To assess the accuracy of the prediction, confidence bounds are added and a goodness-of-fit test is integrated in the R model.

3.2.1. Confidence Bounds

One way to calculate confidence bounds for repairable systems is the Fisher matrix approach, named after Sir Ronald Fisher. The Fisher information is a characteristic commonly used in statistics. It can be defined for a family of probability density functions and can give a declaration about the quality of the parameter estimates for a model. Formally, it is the variance of the score (gradient of the log-likelihood function with respect to the parameter vector) (Ly, Marsman, Verhagen, Grasman, Wagenmakers, 2017). Fisher confidence bounds can be calculated for multiple censored data and are employed in most commercial statistical applications. This method has the advantage of being computationally very simple.

This paper contains the calculation of confidence bounds on the estimation parameters β and λ and the mean cumulative number of failures.

The calculation of the confidence bounds of the estimation parameters by the Fisher matrix approach is performed as following (ReliaSoft, 2010).

Λ is the natural log-likelihood function, shown in Eq. (8).

$$\Lambda = \sum_{q=1}^{K}\left[N_q(ln(\lambda)+ln(\beta)) - \lambda\left(T_q^{\beta} - S_q^{\beta}\right) + (\beta-1)\sum_{i=1}^{N_q}\ln(x_{i,q})\right] \tag{8}$$

All variance can be calculated using the Fisher information matrix in Eq.(9) and implementing Eq. (10) - Eq. (12).

$$\begin{bmatrix} Var(\hat{\lambda}) & Covar(\hat{\beta},\hat{\lambda}) \\ Covar(\hat{\beta},\hat{\lambda}) & Var(\hat{\beta}) \end{bmatrix} = \begin{bmatrix} \frac{\partial^2\Lambda}{\partial\lambda^2} & \frac{\partial^2\Lambda}{\partial\lambda\partial\beta} \\ \frac{\partial^2\Lambda}{\partial\lambda\partial\beta} & \frac{\partial^2\Lambda}{\partial\beta^2} \end{bmatrix}^{-1} \tag{9}$$

with

$$\frac{\partial^2\Lambda}{\partial\beta^2} = -\frac{\sum_{q=1}^{K} N_q}{\beta^2} - \lambda\cdot\sum_{q=1}^{K} T_q^{\beta}\cdot\left(\ln(T_q)\right)^2 \tag{10}$$

$$\frac{\partial^2\Lambda}{\partial\lambda^2} = -\frac{\sum_{q=1}^{K} N_q}{\lambda^2} \tag{11}$$

$$\frac{\partial^2\Lambda}{\partial\lambda\partial\beta} = -\sum_{q=1}^{K} T_q^{\beta}\cdot\ln(T_q) \tag{12}$$

Confidence bounds for β are calculated as shown in Eq. (13), whereas z_α is the α-level's z-score. This value can be extracted from a z table for the defined α-level. The parameter α refers to the likelihood that the true population parameter lies outside the confidence interval. It is usually expressed as a proportion and calculated by *1 - confidence level*. The chosen confidence level in this paper is 90%, therefore $\alpha=0.1$.

$$CB_{\beta} = \hat{\beta}\cdot e^{\pm z_{\alpha}\cdot\sqrt{Var(\hat{\beta})}/\hat{\beta}} \tag{13}$$

Confidence bounds for λ are calculated as shown in Eq. (14).

$$CB_{\lambda} = \hat{\lambda}\cdot e^{\pm z_{\alpha}\cdot\sqrt{Var(\hat{\lambda})}/\hat{\lambda}} \tag{14}$$

The calculation of confidence bounds on the mean cumulative number of failures is shown in Eq. (15) - Eq. (18) (ReliaSoft, 2010).

$$N(t) = \hat{N}(t)\cdot e^{\pm z_{\alpha}\cdot\sqrt{Var(\hat{N}(t))}/\hat{N}(t)} \tag{15}$$

with

$$Var(\hat{N}(t)) = \left(\frac{\partial N(t)}{\partial\beta}\right)^2\cdot Var(\hat{\beta}) + \left(\frac{\partial N(t)}{\partial\lambda}\right)^2\cdot Var(\hat{\lambda}) + 2\cdot\left(\frac{\partial N(t)}{\partial\beta}\right)\cdot\left(\frac{\partial N(t)}{\partial\lambda}\right)\cdot Covar(\hat{\beta},\hat{\lambda}) \tag{16}$$

$$\frac{\partial N(t)}{\partial\beta} = \hat{\lambda}\cdot t^{\hat{\beta}}\cdot\ln(t) \tag{17}$$

$$\frac{\partial N(t)}{\partial\lambda} = \hat{\beta}\cdot t \tag{18}$$

Goodness-of Fit Tests

To test the compatibility of the model and the data statistically, the parametric Cramér-von Mises criterion (ω^2) is often used for the repairable system power law model (Crow, 1982). With this goodness-of fit test, a cumulative distribution function F^* (theoretical distribution) can be compared to a given empirical distribution function F_n (empirically observed function) as shown in Eq. (19).

$$\omega^2 = \int_{-\infty}^{\infty} [F_n(x) - F^*(x)]^2 dF^*(x) \qquad (19)$$

The Cramér-von Mises criterion uses the integral of the squared difference between the empirical and the estimated distribution functions (Parr & Schucany, 1980).

The Cramér-von Mises criterion is appropriate, when the failure data are complete (no gaps between [0, T_q]) and the start time for each system is equal to 0. If these conditions are not met, the general Chi-Squared test, the beta hypothesis test or the Laplace trend test could be applied. As in the presented example of the VGMs the failure data are complete and the start time of all system is 0, the Cramér-von Mises criterion is chosen. The following hypothesis H_1 should be tested.

H_0 := Failure times do not follow a NHPP

H_1 := Failure times follow a NHPP with a failure intensity $u(t) = \lambda \cdot \beta \cdot t^{\beta-1}$

The Cramer-von Mises statistic (C_M^2) is calculated as shown in Eq.(20) (ReliaSoft, 2010).

$$C_M^2 = \frac{1}{12 \cdot M} + \sum_{j=1}^{M} \left(z_j^{\bar{\beta}} - \frac{2j-1}{2 \cdot M} \right)^2 \qquad (20)$$

with the following equations Eq. (21) - Eq. (23).

$$M = \sum_{q=1}^{K} M_q \qquad (21)$$

$M_q = N_q - 1$ (failure-terminated data; $x_{Nqq} = T_q$)

$M_q = N_q$ (time-terminated data; $x_{Nqq} < T$)

$$Y_{iq} = \frac{x_{iq}}{T_q};\ Y_{iq}\ ordered := z_1 < z_2 < \cdots < z_M \qquad (22)$$

$$\bar{\beta} = \frac{M-1}{\sum_{q=1}^{K} \sum_{i=1}^{M_q} ln\left(\frac{T_q}{x_{iq}}\right)} \qquad (23)$$

If the calculated Cramer-von Mises statistic for a given significance level α and the related M is less than the critical value (Table 2), then H_1 is accepted.

Table 2. Critical Values for Cramér-von Mises Test.

	α				
M	**0.20**	**0.15**	**0.10**	**0.05**	**0.01**
2	0.138	0.149	0.162	0.175	0.186
10	0.125	0.142	0.167	0.212	0.32
20	0.128	0.146	0.172	0.217	0.33
30	0.128	0.146	0.172	0.218	0.33
60	0.128	0.147	0.173	0.220	0.33
…	…	…	…	…	…

4. RESULTS OF THE ANALYSIS

The mentioned approach has been performed on the example of the VGMs. This section includes the results of the analysis.

4.1. Rough Failure Analysis

Figure 4 shows an event plot of all the occurred failures per system over time. The figure includes all 39 VGM on the axis of ordinates and their related failure times on the axis of abscissae.

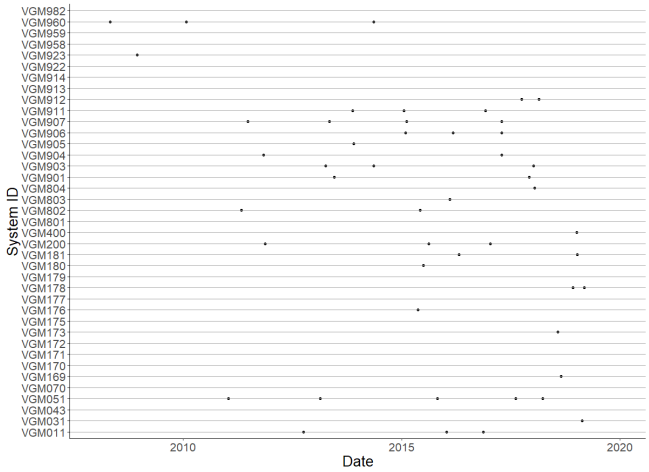

Figure 4: Event Plot of Failures per Unit.

In total, 48 relevant hardware failures occurred (including connector failures) since the installation of the VGMs. The data are right-censored (time-censored); some systems never failed while others failed several times. This has to be considered in the calculation.

It is already interesting to notice from the event plot that the amount of failures increases over time.

In 2013, all power supply modules were exchanged, after several unit failures. The power supply module has a specific lifetime and is therefore excluded from the analysis. All other failure types were analyzed separately in the beginning. The results showed, that the estimation parameters were only slightly different for each failure type. As all growth curves showed a similar behavior, it was possible to analyze them together without hiding details.

4.2. Growth Curve of cumulative number of failures

Figure 5 shows the failure points calculated by the Nelson-Aalen estimator and the estimated parametric growth curve by a power law model over time. The axis of ordinates contains the mean cumulative function (MCF), which describes the cumulative number of failures per unit and on the axis of abscissae the time in hours is shown from 2008 to 2020, total hours (~105k).

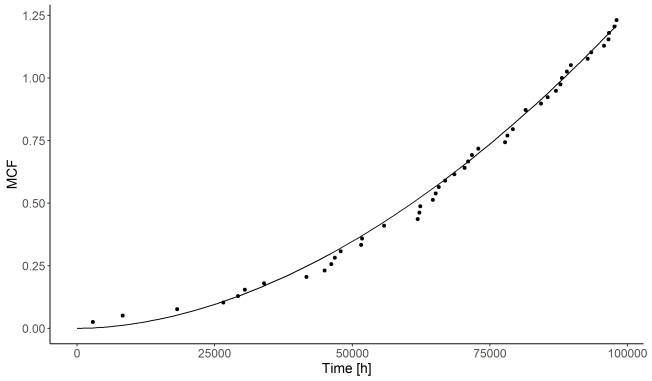

Figure 5: Mean Cumulative Function.

The estimated growth curve is: $\widehat{N}(t) = 6.78 \cdot 10^{-10} \cdot t^{1.85}$ with $\hat{\beta} = 1.85$ and $\hat{\lambda} = 6.78 \cdot 10^{-10}$.

As $\beta > 1$, the systems number of failures is increasing over time and the process is already in the degrading (wear-out) phase.

The instantaneous failure rate of the system (also called instantaneous hazard rate), which is describing the number of failures per hour, is shown in Figure 6.

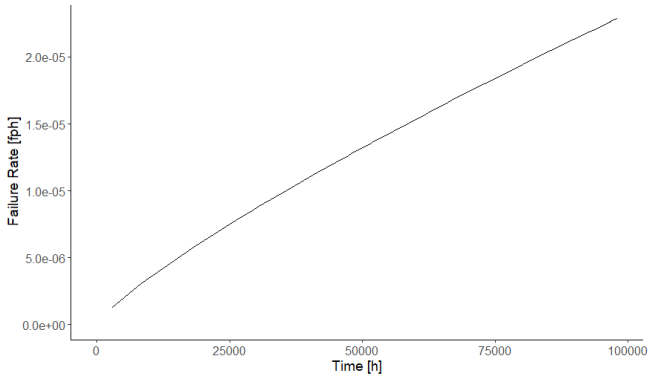

Figure 6: Instantaneous Failure Rate per Unit.

Both graphs show the behavior of a degrading system.

Based on the MCF it is possible to estimate until which time the spare parts are sufficient. Regarding the failure rate one could decide until what time it is still acceptable. Especially for safety critical systems this could be a limiting factor.

4.3. Confidence Bounds and Goodness-of-Fit Results

With the presented Fisher matrix approach, the confidence bounds of the parameter estimations as well as the confidence bounds on the mean cumulative number of failures were calculated.

4.3.1. Confidence Bounds of β and λ

The results of the confidence bounds of β and λ with $\alpha = 0.1$ are the following:

Fisher:

$CB_{\beta\_lower} = 1.46, \qquad CB_{\beta\_upper} = 2.35$

$CB_{\lambda\_lower} = 4.27 \cdot 10^{-12}, \; CB_{\lambda\_upper} = 1.08 \cdot 10^{-7}$

Crow:

$CB_{\beta\_lower} = 1.44, \qquad CB_{\beta\_upper} = 2.31$

$CB_{\lambda\_lower} = 5.26 \cdot 10^{-10}, \; CB_{\lambda\_upper} = 8.63 \cdot 10^{-10}$

As, for both methods, β is always larger than one, even for the lower bounds, it can be concluded, that the system is certainly in the wear-out phase and the failure rate will increase in the future exponentially. The system is not in the constant phase of its lifetime anymore.

4.3.2. Confidence Bounds on Mean Cumulative Function

Figure 7 shows the estimated mean cumulative number of failures with Fisher confidence bounds with $\alpha = 0.1$. The growth curve is extrapolated until 01/01/2027 (166560h).

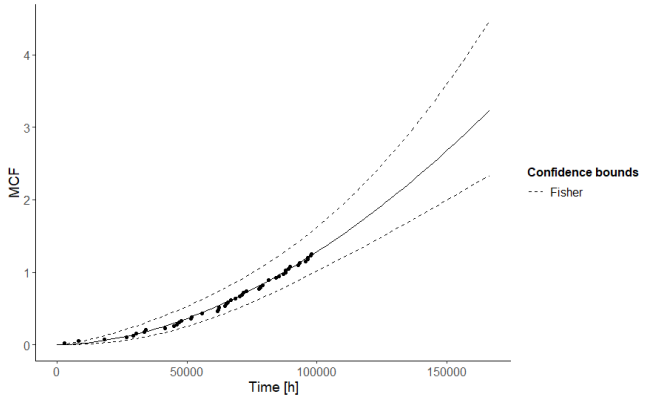

Figure 7: Mean Cumulative Function with Confidence Bounds.

When extrapolating the growth curve, an estimation about the number of failures at a certain point in the future can be made. As for the VGM the number of spare parts is limited, this graph can help to plan the exchange of the system.

4.3.3. Cramér-von Mises Test Statistic

The result for the Cramér-von Mises statistic is $C_M^2 = 0.058$.

For a significance level of $\alpha=0.1$ and $M=48$, the Cramer statistic is lower than the critical value (0.172) and H_1 can be accepted.

Table 3: Cramér-von Mises Values

	α				
M	**0.20**	**0.15**	**0.10**	**0.05**	**0.01**
…	…	…	…	…	…
30	0.128	0.146	0.172	0.218	0.33
60	0.128	0.147	0.173	0.220	0.33
…	…	…	…	…	…

It can be concluded that the data follows a non-homogeneous Poisson process with a power law failure intensity.

4.4. Cost Estimation and Optimal Maintenance Strategy

For each failure type, the repair costs are known from the invoices of the external company. Considering this, the MCF can be expanded by the costs and the cumulative normalized repair costs per system can be plotted (Figure 8).

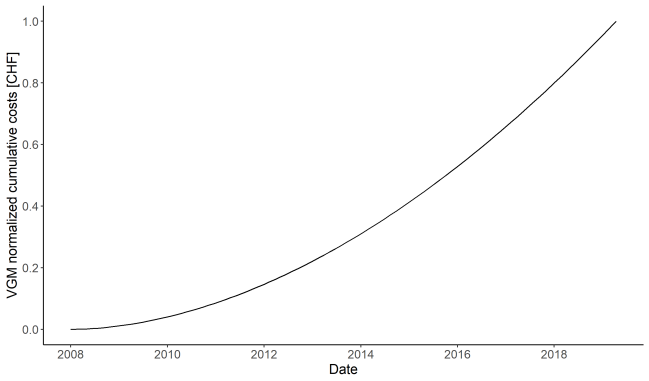

Figure 8: Cumulative Normalized Repair Costs per System Unit.

This estimation helps to plan the budget and maintenance and to find the optimal point to replace the system by a new one. As a rough estimate, this point is reached when the cumulative costs are equal to the asset costs of a new system.

5. CONCLUSION & OUTLOOK

From the statistical approach, it can be concluded that the VGM system is already in its degrading mode and the failure rate is increasing over time. The current failure rate is $2.3 \cdot 10^{-5}$ failures per million hours *[fpmh]*. The replacement for the VGMs is foreseen between 2027 and 2031. There the instantaneous failure rate per system would be $3.6 \cdot 10^{-5}$*[fpmh]* and $4.2 \cdot 10^{-5}$*[fpmh]* respectively.

As spare parts are limited, the application of this system is restricted. This is the most critical point that should be considered when planning the exchange time. The extrapolation of the MCF helps to identify the time, where the maximum amount of failures occurred which can be replaced by components in stock. Regarding the VGMs the current cumulative number of failures is *1.23* per system unit. In 2027 and 2031 it would be *3.23* per system unit and *4.61* respectively. This number contains all types of failures that have occurred.

Regarding the repair costs, the results show that it is recommendable to wait until 2031 to exchange the system.

The presented approach will be applied to other monitoring systems as well. Generally, the results of this analysis help to identify where the system is located in its lifetime curve, to estimate lifetime cost, to schedule maintenance and to plan the replacement of the system.

ACKNOWLEDGEMENT

Many thanks are due to Julien Regnard for providing the data used for this analysis. We also thank Fabrice Malacrida for the intellectual discussions and his technical feedback concerning the VGM operating mode.

NOMENCLATURE

fpmh	failures per million hours
HPP	Homogeneous Poisson Process
MCF	Mean Cumulative Function
NHPP	Non-homogeneous Poisson Process
SIL	Safety Integrity Level
VGM	Ventilation Gas Monitor

REFERENCES

Birolini, A. (2017). *Reliability Engineering. Theory and Practice.* Zurich, Switzerland: Springer

Crow, L.H. (1974). *Reliability Analysis for Complex, Repairable Systems in Reliability and Biometry*. Philadelphia, Pennsylvania: Society for Industrial and Applied Mathematics (SIAM)

Ferragut, A. (2005). *Spécifications techniques: Mesure des gaz Radioactifs «ASGA».* Technical specification. Assystem, France

Ly, A., Marsman, M., Verhagen, J., Grasman, R., Wagenmakers, E.-J. (2017). *A Tutorial on Fisher Information.* Amsterdam, Netherlands. arXiv:1705.01064 [math.ST]

Nelson, W. (2003). *Recurrent Events Data Analysis for Product Repairs, Disease Recurrences, and Other Applications*. Philadelphia, Pennsylvania: ASA-SIAM Series on Statistics and Applied Probability

Parr, W. C.; Schucany, W. R. (1980). Minimum Distance and Robust Estimation. *Journal of the American Statistical Association*. vol. 75, pp. 616–624. doi:10.1080/01621459.1980.10477522

Perrin, D. (2018). *Introduction to CERN Radiation Monitoring System*. Presentation Satellite Workshop. CERN, Genève, Switzerland

ReliaSoft Corporation. (2010). *Reliability Growth & Repairable System Data Analysis Reference.* Tucson, Arizona: ReliaSoft Corporation

BIOGRAPHIES

Saskia Hurst was born 1990 in Munich. She holds a Bachelor degree in Industrial Engineering (ESB Business School Reutlingen, Germany, 2013) and a Master degree in Technology Management (University of Stuttgart, Germany, 2017). She is currently working for the radiation protection group at CERN as a reliability engineer. Her areas of expertise are RAMS analysis for safety systems, SIL verification and statistical analysis.

H. Boukabache is a project leader at CERN working for the radiation protection group. He is currently leading a team in charge of the development and the manufacturing of the new generation of CERN ionizing radiation monitoring system. His main researches focus on System on Chip development, ultra-low current measurement techniques and hardening methods for safety critical systems.

He obtained his PhD degree in Micro and Nano-Systems in 2013 and he got many awards for his work with Aerospace companies and the French National Center for Scientific Research (CNRS) on heterogeneous aircraft structural health monitoring. He obtained his master degree in electronic and automatic control from the French Institute of Applied Science at Toulouse in 2009. He also obtained in the same year a second master degree in micro technology from the University of Toulouse in France.

D. Perrin was born in 1963 in France. After receiving a diploma in electronics from the University Institute of Technology of St-Etienne in 1983 he worked for CERN as an Electronics Technical Engineer for the development of the control units of the electrostatic separators for the Large Electron-Positron (LEP) collider. In 1992 he joined the CERN Radiation Protection Group for which he designed and developed instrumentation for ionizing radiation measurement. Since 2001 he is Head of the Instrumentation & Logistics Section of the CERN Radiation Protection Group. He led projects for the design and the supply of the radiation monitoring system for the Large Hadron Collider (LHC) and the injector chain. Since 2013 he manages the RAdiation Monitoring System for the Environment and Safety (RAMSES) Program at CERN.